Cyclic Cis Vicinal Tertiary Diamines: Structure, Conformational Dynamics, and Proton Transfer

Gideon Fraenkel,* Vaidyanathan Balasubramanian, Hyejin Lisa Chang, and Judith Gallucci

Contribution from the Chemistry Department, The Ohio State University, Columbus, Ohio 43210

Received January 4, 1993

Abstract: Carbon-13 NMR line-shape analysis of several cyclic (cyclohexenes and cyclopentanes) cis vicinal tertiary diamines with *N*-piperidino or *N*-pyrrolidino substituents reveals barriers to cyclohexane inversion ($\Delta H^{\ddagger}$) of 10–11 kcal/mol with $\Delta S^{\ddagger}$ = 6–8 eu, while for piperidine inversion $\Delta H^{\ddagger}$ = 10–12 kcal/mol with a $\Delta S^{\ddagger}$ of 2–9 eu. All cis diamines studied exhibited two pK_a's, the first 10–11 and the second 3–5. The crystal structure of *cis*-1,2-bis(*N*,*N*-dimethylamino)cyclopentane monopicrate, **1**-picrate, shows the diamine, **1**, to be unsymmetrically protonated, the acid proton–nitrogen distances being 2.56 and 0.93 Å; the entire assembly of O⁻(picrate), acid proton, and two nitrogens is almost coplanar, with H^+ just 0.04 Å out of the O⁻(picrate), N, N^+ plane. The cyclopentane forms a half-chair in which the carbons *C*–N^+ and *C*–N lie, respectively, 0.32 and 0.28 Å on opposite sides of the three-methylene-carbon plane. Carbon-13 NMR of several salts of **1** in CD_2Cl_2 shows that proton transfer between nitrogens within the cation is fast down to 200 K, while reversible transfer of this proton to counterion is much slower. Activation parameters for nitrogen inversion in the monotrifluoroacetate of **9**, found from ^{13}C NMR line-shape analysis to be $\Delta H^{\ddagger}$ = 22 kcal/mol and $\Delta S^{\ddagger}$ = 34 eu, imply that fast reversible transfer of a proton between cation and anion is rate determining to nitrogen inversion.

Cyclic cis vicinal tertiary diamines, a hitherto neglected class of theoretically interesting and potentially physiologically active compounds,[1] are not well-known due to the absence, until recently, of efficient procedures to make them.[2] These compounds are potentially important as ligands for metal ions (Li^+, Mg^{2+}, Ca^{2+}), as catalysts for the reactions of organolithium compounds,[3] and in Pt^{II} complexes, of utility in cancer therapy.[4] Recently a cis vicinal tertiary diamino substituted cyclohexane was reported to complex strongly and selectively to the σ receptor in the guinea pig brain.[6]

Our recent synthesis of several cyclic cis vicinal tertiary diamines[2] **1–5** has rendered these compounds conveniently available for study. This paper describes investigations of structure, conformational dynamics, and proton-transfer phenomena.

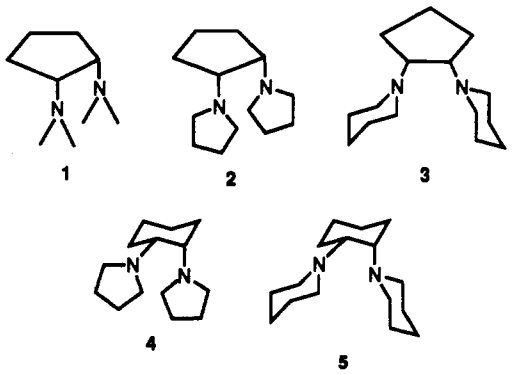

Results and Discussion

Under conditions of slow nitrogen inversion and slow rotation around the N–C(ring) bond, compounds **1** and **2** might be expected to exhibit diastereotopic shifts in ^{13}C and proton NMR due to chirality at the carbinyl carbons. Then **1** would give rise to two N–CH_3 (^1H and ^{13}C) resonances of equal intensity, and **2** should show an equal doublet for ^{13}C NMR of CH_2N. In fact, all methyl carbons of **1** in cyclopentane-d_2 are magnetically equivalent between 300 and 150 K as are all NCH_2 carbons of **2**, also in cyclopentane-d_2. Either these proposed shifts are too small to observe or, alternatively, the inversion–rotation processes are fast relative to the corresponding frequency shifts, even at 150 K.

Consistent with the proposed chair cyclohexane structure, both the cis 1,2-disubstituted cyclohexanes **4** and **5** show nonequivalent carbinyl carbons at low temperature, 150 K, in ^{13}C NMR, separated by *ca.* 10 ppm. With increasing temperature these doublets progressively signal average due to faster chair–chair interconversion of the cyclohexane ring (1). NMR line-shape

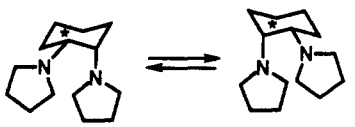

(1)

analysis[6] of the ^{13}C carbinyl resonance provides activation parameters for the chair–chair interconversion of the cyclohexane. Furthermore, in **3** and **5** ^{13}C NMR line-shape due to CH_2N of piperidino substituents provides dynamic data for piperidine ring flipping and inversion at nitrogen; examples follow below in order of increasing complexity.

Consider first compound **3**. Carbon-13 NMR (cyclopentane-d_2 solution), Figure 1, of the cyclopentane moiety is essentially invariant with temperature. At 200 K the two piperidino rings exhibit the same set of five ^{13}C resonances of equal intensity; the nonequivalence of the C_α carbons and C_β carbons in the two piperidine rings is most likely due to chirality at carbinyl carbons. We shall assume throughout this paper that piperidino groups

(1) Levine, S.; Sowinski, R. *Am. J. Pathol.* **1982**, *107*, 135–141.
(2) Fraenkel, G.; Gallucci, J.; Rosenzweig, H. S. *J. Org. Chem.* **1989**, *54*, 677–681.
(3) Langer, A. W. *Trans. N. Y. Acad. Sci. Ser. 2* **1965**, *27*, 741.
(4) (a) Penta, J. S.; Maggia, F. M.; Salem, P. A. In *Cancer Chemotherapy 1*; Maggia, F. M., Ed.; Magnius Nighoff Publishers: The Hague, 1983; pp 149–169. (b) Crooke, S. P. In *Cis-Platin, Current Status and New Developments*; Prestayko, A. W. X., Carter, S. K. Eds.; Academic Press: New York, 1980. (c) Scovel, W. M.; Kroos, L. R. *Biochem. Biophys. Res. Commun.* **1982**, *108*, 16. (d) Lund, T.; Toftlund, A. *Acta Chem. Scand.* **1982**, *A36*, 489.
(5) de Costa, B. R.; Bowen, W. D.; Hellewell, S. B.; George, C.; Rothman, R. B.; Reid, A. A.; Walker, J. M.; Jacobson, A. E.; Rice, K. C. *J. Med. Chem.* **1989**, *32*, 1996–2002.
(6) Kaplan, J. I.; Fraenkel, G. *NMR of Chemically Exchanging Systems*; Academic Press: New York, 1980; Chapter 6.

0002-7863/93/1515-6795$04.00/0

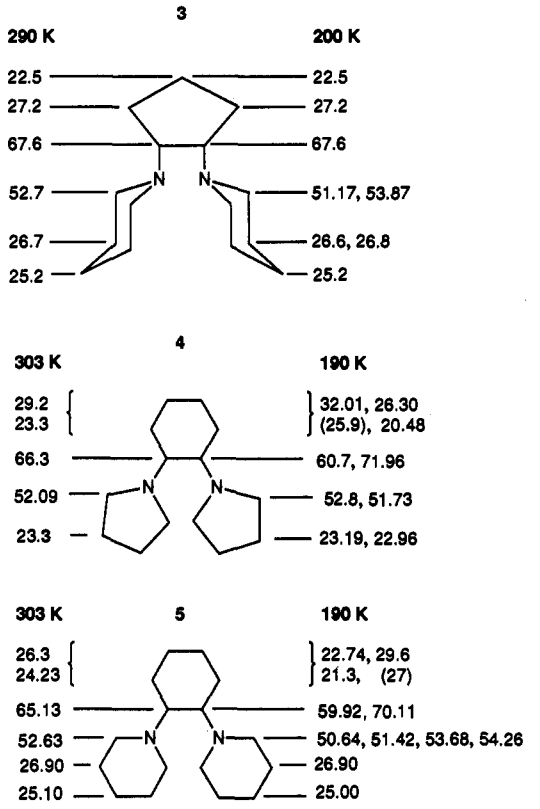

Figure 1. ^{13}C NMR of **3**, **4**, and **5** in cyclopentane-d_2, shifts at two temperatures, δ units.

take the chair structure[7,8] and that the large substituent on nitrogen will always be equatorial[9] as amply established by Lambert.

Above 200 K, with increasing temperature there is signal averaging of the two C_α ^{13}C piperidine resonances of **3** as well as of the C_β resonances; see Figures 1 and 2. Line-shape analysis of the C_α collapsing doublet provides the rates of interconversion and, in turn, the Eyring plot in Figure 3 with $\Delta H^\ddagger = 12.4$ kcal/mol and $\Delta S^\ddagger = 2.5$ eu. These effects must be the collective result of inversion at nitrogen, rotation around the *N*–CH(ring) bond, and inversion of the piperidine ring; see Scheme I. The above activation parameters apply to piperidine inversion since this process is by far the slowest of the three. For example, $\Delta G^\ddagger$ values for nitrogen inversion and ring inversion in piperidine were reported to be 7.8 and 10.4 kcal/mol,[10] respectively; the corresponding values for *N*-methylpiperidine were 8.7 and 12.1 kcal/mol,[9a-11] respectively.

Carbon-13 NMR of **4** at 190 K shows nonequivalent carbinyl carbons separated by *ca.* 11 ppm, confirming the cis vicinal structure as reported previously;[2] see Figure 1. Above 190 K this doublet undergoes signal averaging; see Figure 4. Comparison of experimental and calculated line shapes provided the rates of cyclohexane inversion, and from the Eyring plot in Figure 5 were

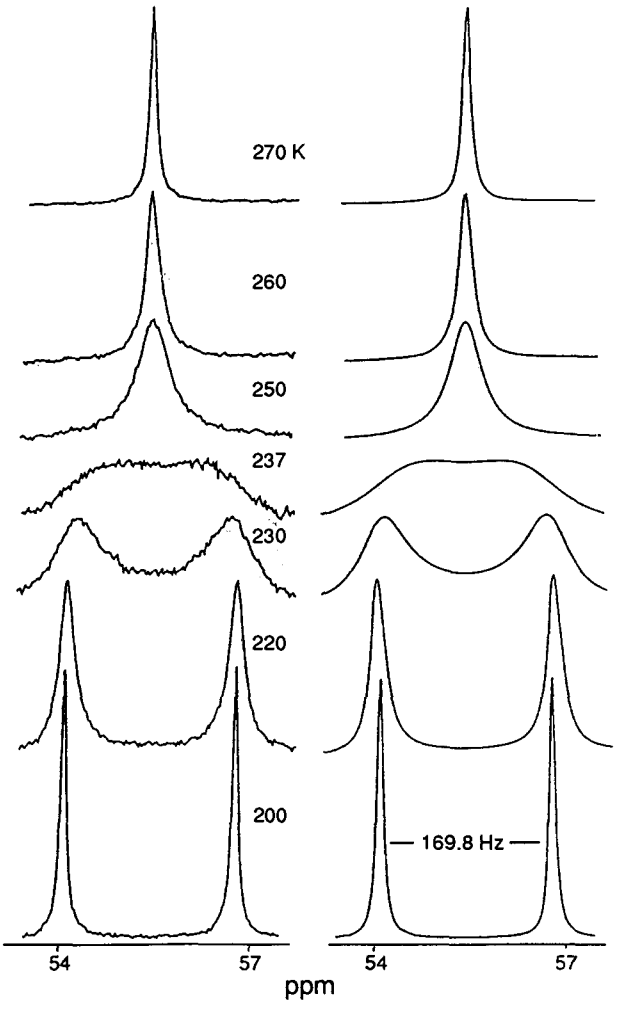

Figure 2. ^{13}C NMR of **3** in cyclopentane-d_2, CH_2N line shapes: (left) observed, different temperatures; (right) calculated.

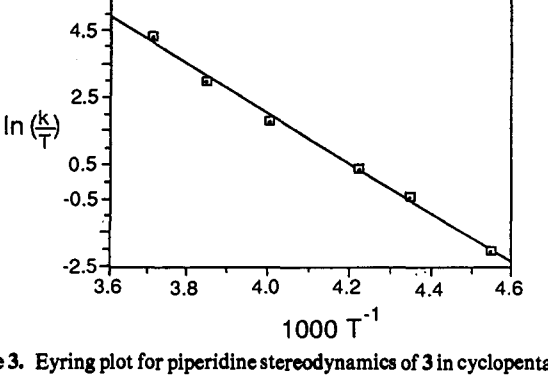

Figure 3. Eyring plot for piperidine stereodynamics of **3** in cyclopentane-d_2.

obtained activation parameters $\Delta H^\ddagger$ and $\Delta S^\ddagger$ of respectively 12.4 kcal/mol and 2.5 eu.

Carbon-13 line-shape changes for C_3, C_4, C_5, and C_6 of the cyclohexane ring in **4** are also quantitatively indicative of ring inversion dynamics. Sharp peaks are observed at 190 K at 32.01 and 20.48 δ. With increasing temperature these resonances broaden and disappear into the base line. By 280 K one new peak appears at 29.1 δ. Most likely the latter is the result of averaging the 32.01 δ resonance with one seen as a shoulder on the solvent (cyclopentane-d_2) resonance at 26.3 δ. In similar fashion the peak at 20.48 δ must be the upfield line of a second equal doublet whose deshielded component lies just below solvent absorption between 25 and 26 δ. The averaged resonance for this doublet would be coincident with the peak at 23.3 δ due to NCH_2CH_2.

(7) (a) Przybylska, M.; Barnes, W. H. *Acta Crystallogr.* **1953**, *6*, 377. (b) Visser, J. W.; Manneson, J.; De Vries, J. L. *Ibid.* **1954**, *7*, 288. (c) Lambert, J. B. *J. Am. Chem. Soc.* **1967**, *89*, 1836.

(8) Reviews: (a) Lambert, J. B.; Featherman, S. I. *Chem. Rev.* **1975**, *5*, 611. (b) Rubiralta, M.; Giralt, E.; Diez, A. *Piperidine Structure Preparation, Reactivity and Synthetic Applications of Piperidine and its Derivatives*; Elsevier: Amsterdam, 1991. (c) Delpeuch, J. J. *Cyclic Organonitrogen Stereodynamics*; Lambert, J. B., Takeuchi, Y. Eds.; VCH: New York, 1992; pp 169–180.

(9) (a) Lambert, J. B.; Keske, R. G. *J. Am. Chem. Soc.* **1966**, *88*, 620. (b) Lambert, J. B.; Keske, R. G.; Cahart, R. E.; Jovanovitch, A. P. *J. Am. Chem. Soc.* **1967**, *89*, 3761. (c) Baldock, R. W.; Katritzky, A. R. *J. Chem. Soc. B* **1968**, 1470.

(10) (a) Anet, F. A. L.; Yavari, I. *J. Am. Chem. Soc.* **1977**, *99*, 2794. (b) Baldock, R. W.; Katritzky, A. R. *J. Chem. Soc. B* **1968**, 1470.

(11) (a) Crowley, P. J.; Robinson, N. J. T.; Ward, M. G. *J. Chem. Soc., Chem. Commun.* **1974**, 825. (b) Crowley, P. J.; Robinson, N. J. T. *Tetrahedron* **1977**, *33*, 915. (c) Gittins, V. M.; Heywood, P. J.; Wyn-Jones, E. J. *J. Chem. Soc., Perkin Trans. 2* **1975**, 1642.

Scheme I [a]

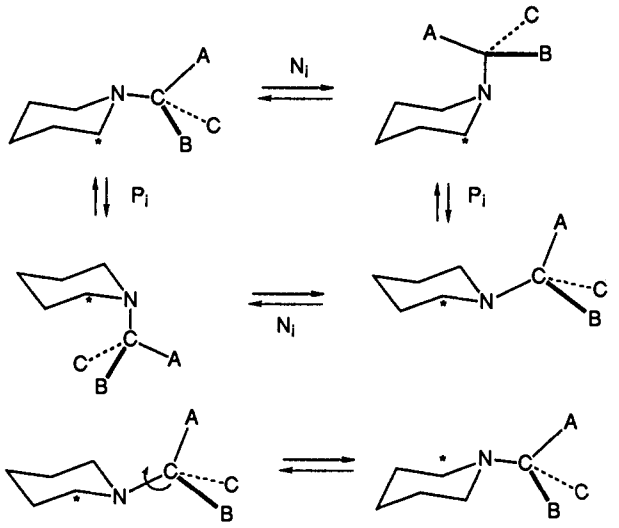

[a] P_i, piperidine inversion; N_i, nitrogen inversion.

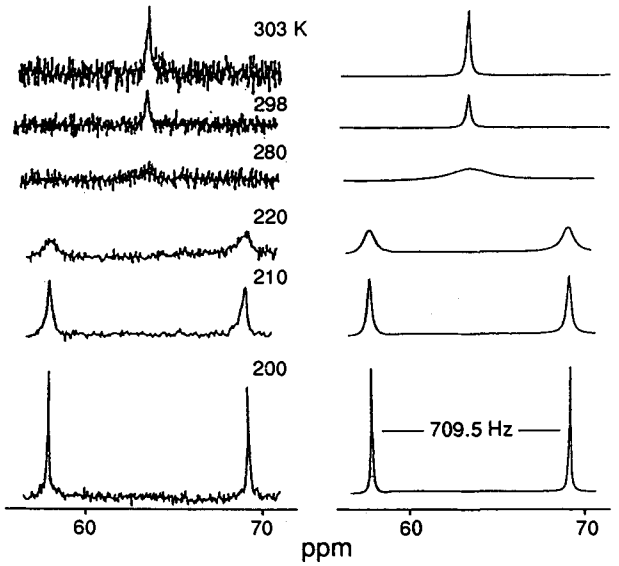

Figure 4. ^{13}C NMR line shapes of carbinyl carbons of **4** in cyclopentane-d_2: (left) observed, different temperatures; (right) calculated.

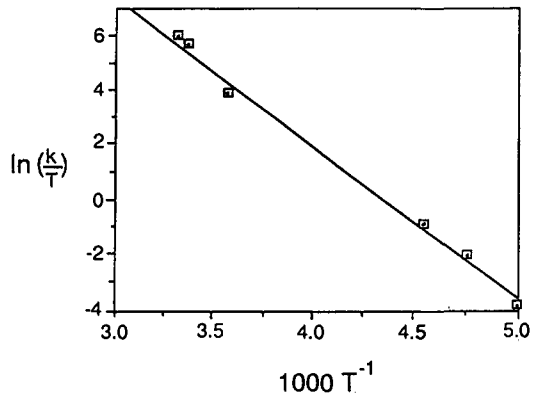

Figure 5. Eyring plot for cyclohexane ring inversion in **4** in cyclopentane-d_2 solution.

Actually, just the base of this otherwise narrow resonance is quite broad at 280 K. The most reasonable interpretation of these observations is that C_3/C_6 and C_4/C_5 of the cyclohexane ring each give rise to one of these proposed low-temperature doublets and that the signal averaging comes from the dynamics of cyclohexane inversion.

In principle, under conditions of slow inversion at nitrogen, slow cyclohexane inversion, and slow rotation around the N–CH bond, all pyrrolidine carbons in **4** should be magnetically nonequivalent. At 190 K the NCH_2CH_2 carbon resonance resolved into a narrowly spaced doublet (0.23 ppm), while that for NCH_2 consists of two lines, one broad (52.8 δ) and the other sharp (51.73 δ). Below 190 K the sample freezes. Thus, either the diastereomeric shifts or those due to axial vs equatorial sites are too small to resolve or one or more of these rate processes is fast enough to average these shifts even partially. Thus, one can qualitatively observe the effects of these inversion processes but not measure their rates.

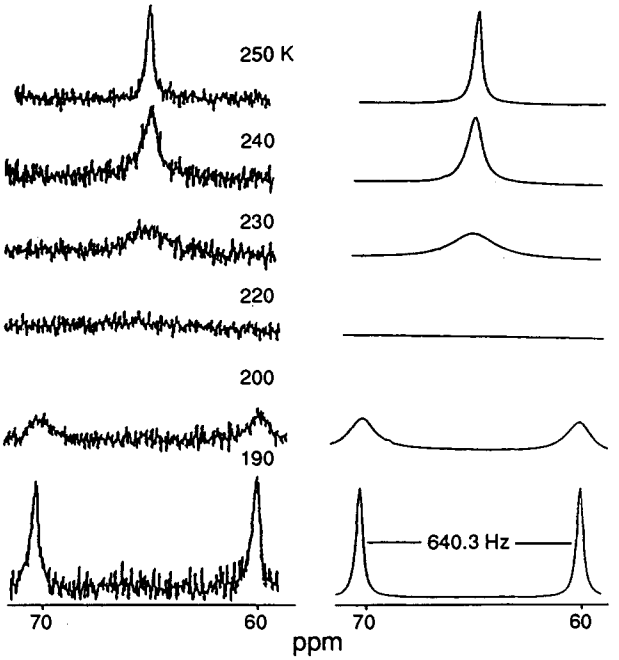

Figure 6. ^{13}C NMR, carbinyl line shapes of **5** in cyclopentane-d_2: (left) observed, different temperatures; (right) calculated.

In the case of **5**, two dynamic processes have been investigated from the NMR line shapes. The carbinyl ^{13}C resonance at 190 K consists of a well-defined 1:1 doublet which, with increasing temperature, progressively undergoes signal averaging; see Figure 6. Line-shape analysis provides the rate constants for cyclohexane inversion and accompanying activation parameters, $\Delta H^{\ddagger}$ and $\Delta S^{\ddagger}$, of respectively 11.4 kcal/mol and 2.6 eu.

Changes in the ^{13}C NMR line shape of C_3, C_4, C_5, and C_6 of the cyclohexane ring in **5** are also the result of ring inversion dynamics. Resonances observed at 190 K at 29.6, 22.74, and 21.32 δ 1:1:1 signal-average by 270 K to an equal doublet at 26.3 and 24.32 δ. Then assuming intrinsic shifts change little with temperature, we assign the 22.74/29.6 δ doublet to average at 26.3 δ. For the second doublet to average at 26.3 δ, one peak is at 21.3 δ and the other must be obscured by solvent cyclopentane-d_2 at 27 δ. Thus, one collapsing doublet comes from C_3/C_6 and the other from C_4/C_5. No further assignment can be made, as in the case of compound **4**.

Changes in the ^{13}C NMR of the NCH_2 carbons of **5** provide inversion rates for both cyclohexane and piperidine moieties. In the rigid molecule, **5**, all NCH_2 carbons should be magnetically nonequivalent due to chirality at the carbinyl carbons and taking into account the axial and equatorial environments of the substituents. Actually, at 190 K there are four lines of equal intensity for NCH_2. With increasing temperature these average to a single line at 52.63 δ by 270 K. The diastereotopic shift between NCH_2 carbons within a piperidine ring would be averaged under conditions when rotation around the N–CH bond, inversion at nitrogen, and inversion of the piperidine ring are all fast, relative to the frequency separations among the *N*-methylene carbon shifts. Final averaging of the resulting two peaks, one for each piperidine

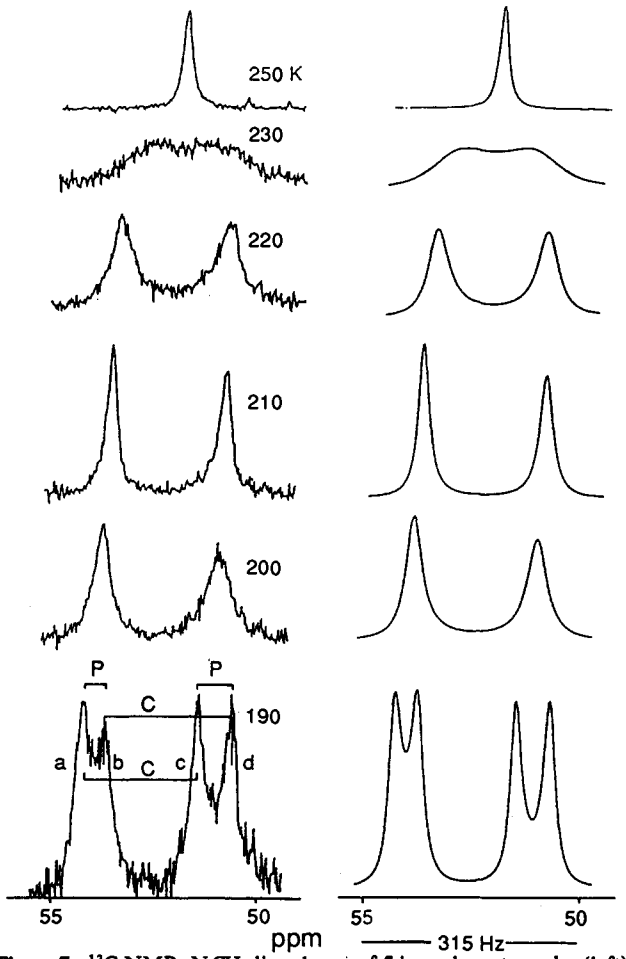

Figure 7. ^{13}C NMR, NCH_2 line shapes of **5** in cyclopentane-d_2: (left) observed, different temperatures; (right) calculated; P brackets signals averaged by piperidine inversion; C brackets signals averaged by cyclohexane inversion.

ring, would be due to fast inversion of the cyclohexane ring. Inspection of the spectra, Figure 7, reveals the pattern of signal averaging as indicated by the diagram at the bottom of the figure. The density matrix equations required to solve for the NCH_2 ^{13}C NMR line shape, which take into account the piperidine and cyclohexane inversion processes, are shown in matrix form in eq 2, wherein $\Delta\omega_i$ is $\omega - \omega_i$, shifts in the rotating frame; $1/T$ is line width; ρ^i are half spin elements of the density matrix; c is a constant; and k's are rate constants for cyclohexane inversion, k_c, and piperidine inversion k_p. Then absorption is obtained from the sum in eq 3 Comparison of experimental with calculated line

$$\begin{bmatrix} i\Delta\omega_a - 1/T - k_p - k_c & k_p & k_c & 0 \\ k_p & i\Delta\omega_b - 1/T - k_p - k_c & 0 & k_c \\ k_c & 0 & i\Delta\omega_c - 1/T - k_p - k_c & k_p \\ 0 & k_c & k_p & i\Delta\omega_d - 1/T - k_p - k_c \end{bmatrix} \begin{bmatrix} \rho^a \\ \rho^b \\ \rho^c \\ \rho^d \end{bmatrix} = iC \begin{bmatrix} 1 \\ 1 \\ 1 \\ 1 \end{bmatrix} \quad (2)$$

$$\mathrm{Abs}(\omega) = -\mathrm{Im}(\rho^a + \rho^b + \rho^c + \rho^d) \quad (3)$$

shapes gives rise to the Eyring plot shown in Figure 8. The resulting activation parameters are listed in Table I together with those from compounds **3** and **4**. The $\Delta H^\ddagger$ barriers to chair–chair interconversion in the cyclohexane moieties of **4** and **5**, in the

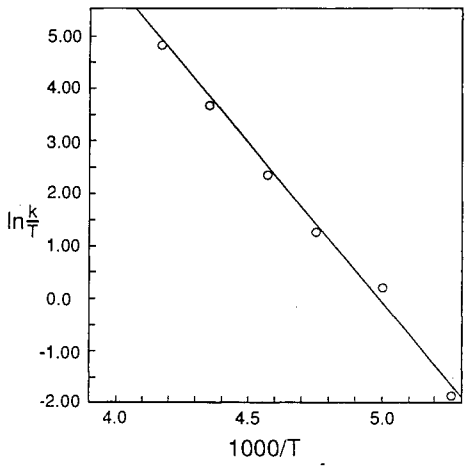

Figure 8. Eyring plot for piperidine inversion in **5**.

Table I. Activation Parameters for Ring Inversion in Cyclic Cis Vicinal Tertiary Diamines

compd	inversion	^{13}C res	$\Delta H^\ddagger$ (kcal/mol)	$\Delta S^\ddagger$ (eu)
3	pip[a]	CH_2N	12.4	2.5
4	cyc[b]	CH	11	−0.9
5	cyc[b]	CH	11.3	8.8
5	pip[a]	CH_2N	10.1	8.9

[a] Piperidine. [b] Cyclohexane.

neighborhood of 11 kcal/mol, are quite similar to published values for substituted cyclohexanes.[12] As noted above, in the case of the piperidino moieties, averaging of the ^{13}C CH_2N diastereotopic shift takes place when rotation around the N–CH bond, inversion at nitrogen, and piperidine ring inversion are all fast, relative to the NMR time scale. By analogy to published results, under our conditions the rates of the first two processes would be too fast to measure using NMR line-shape analysis. Hence, the measurements in this work must apply to the slowest of these processes, ring inversion of the piperidine moiety. Our values closely resemble published results for a variety of piperidines.[9a,b,10a,13–15] Interestingly, we find both kinds of ring inversion, cyclohexane and piperidine moieties, to exhibit very similar enthalpies of activation.

Questions concerning mode of protonation of a cyclic cis vicinal diamine include whether it is symmetrical, **6**, and if not, **7**, what is the nature of the intramolecular hydrogen bond, N^+–H···N?

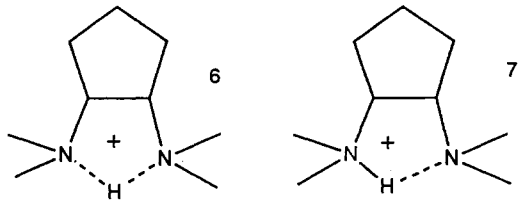

We have previously reported the crystallographic structure of the dipicrate of **3**.[2] The one O^- and two N^+H moieties form a triple-ion assembly. In addition, the dication is distorted due to repulsion between the nitrogens as evidenced by the large N^+–C–C–N^+ dihedral angle of 58°. We have now determined the structure of the monopicrate of **1** by X-ray crystallography. This

(12) Summarized in the following: Anet, F. A. L. *Dynamic Nuclear Magnetic Resonance Spectroscopy*; Jackman, L. M., Cotton, F. A., Eds.; Academic Press: New York, 1975; pp 582–583.
(13) (a) Yousif, G. A.; Roberts, J. D. *J. Am. Chem. Soc.* **1968**, *90*, 6428. (b) Lambert, J. B.; Bailey, D. S.; Michel, B. F. *J. Am. Chem. Soc.* **1972**, *94*, 3812. (c) Delpeuch, J. J.; Deschamps, M. N. *Chem. Commun.* **1967**, 1188.
(14) Reference 8c, pp 236–238.
(15) Summarized in ref 12, p 587.
(16) Bucourt, R. *Topics in Stereochemistry*; Eliel, E. L., Allinger, N. L., Eds.; Wiley-Interscience: New York, 1974; Vol. 8.

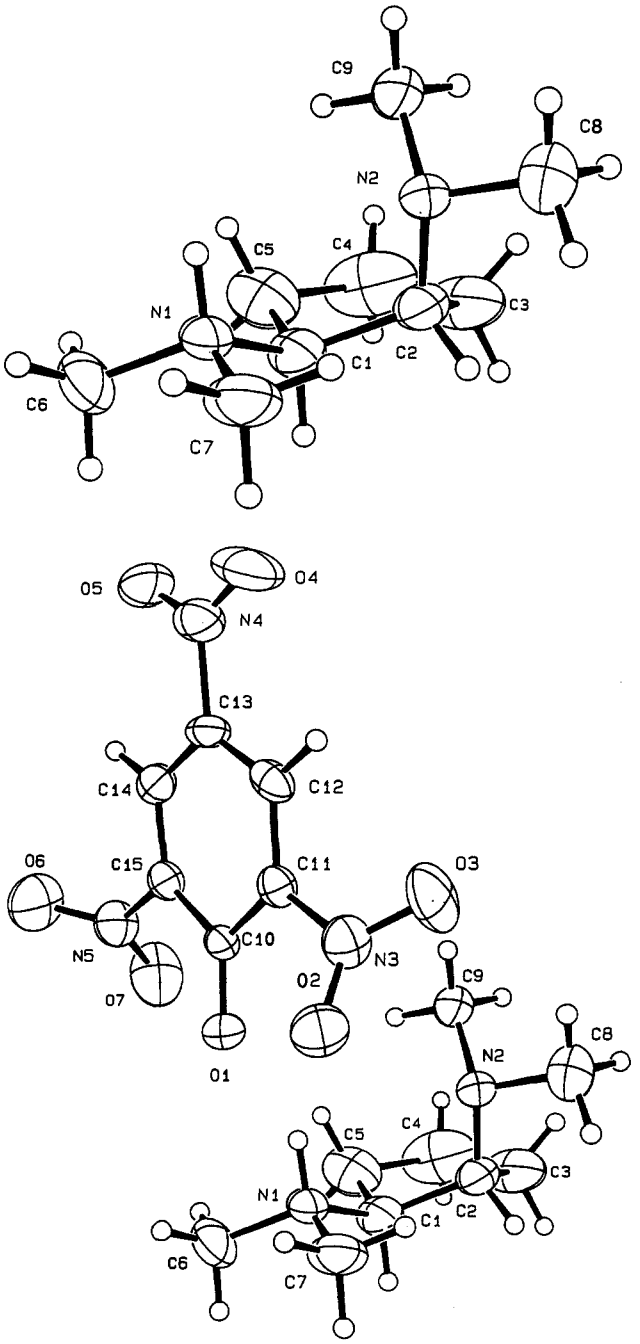

Figure 9. ORTEP diagram, crystallographic structure of **1**-picrate. The non-hydrogen atoms are drawn with 30% probability thermal ellipsoids. Hydrogen atoms are drawn with an arbitrary radius. (Top) Cation alone. (Bottom) Both ions.

study reveals the mode of protonation to be quite unsymmetrical; see Figure 10 and Table II.

The torsional angles for the cyclopentane ring, see Table II, are very close to those for an idealized half-chair, **8**.[16] In **1**-picrate

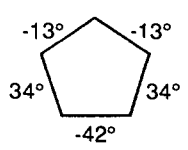

8

the C_1–N^+ and C_2–N carbons lie respectively 0.32 and 0.28 Å on opposite sides of the three-methylene-carbon plane, C_3, C_4, and C_5. As seen in Figure 9, C_1–N_1^+ is pseudoequatorial and C_2–N is pseudoaxial. The dihedral angle between them is −35.5 (looking from C_1 to C_2).

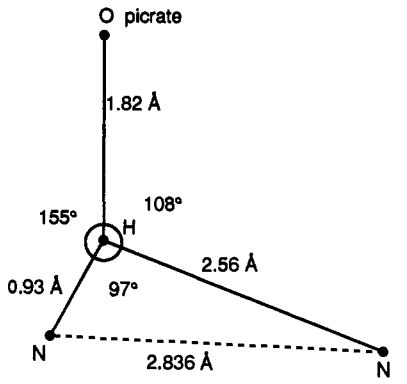

Figure 10. Structure around the acid proton in **1**-picrate.

Table II. Selected Structural Parameters, **1**-Picrate

	Bond Lengths (Å)		
C_1 C_2	1.530(8)	C_5 C_1	1.521(9)
C_2 C_3	1.535(10)	C_1 N_1	1.484(7)
C_3 C_4	1.506(13)	C_2 N_2	1.455(8)
C_4 C_5	1.553(12)	N_1 H_3	0.93(5)
	Bond Angles (deg)		
C_1 C_2 C_3	101.2(7)	N_1 C_1 C_2	113.7(6)
C_2 C_3 C_4	108.1(7)	N_1 C_1 C_5	113.4 (6)
C_3 C_4 C_5	106.5(8)	N_2 C_2 C_1	113.9(5)
C_1 C_5 C_4	103.9(7)	N_2 C_2 C_3	118.3(6)
C_2 C_1 C_5	106.2(6)	N_1 H_3[a] N_2	97(4)
	Torsional Angles (deg)		
C_1 C_2 C_3 C_4	29.9(8)	C_3 C_2 C_1 C_5	−38.0(7)
C_1 C_5 C_4 C_3	−12.5(9)	N_1 C_1 C_2 N_2	−35.5(8)
C_2 C_1 C_5 C_4	31.8(7)	N_1 C_1 C_5 C_4	+157.4(6)
C_2 C_3 C_4 C_5	−11(1)	N_2 C_2 C_3 C_4	−95.1(9)

[a] Acid proton.

The C_1–N_1^+ bond of 1.484 Å is significantly longer than the C_2–N bond, 1.455 Å. This lengthening was observed in the crystallographic structure of *trans*-1,2-diaminocyclohexane monohydrobromine[17] and is also well documented in the literature,[18] average bond lengths for C_{sp3}–N^+ and C_{sp3}–N being 1.499 and 1.469 Å, respectively.

The position of the hydrogen atom bonded to N_1 of **1**-picrate is believed to be correct since the positional and thermal parameters converged to reasonable values during least squares refinement. The geometry about N_1^+ is tetrahedral, as expected, and the refined position of the hydrogen atom is very close to its original position as located on a difference electron density map.

As indicated above and in Figure 9, the diamine is unsymmetrically protonated with an acid proton, which is hydrogen bonded to O^- of picrate and much closer to N_1 (0.93 Å) than to N_2 (2.56 Å); see Figures 9 and 10. The entire assembly of O^-(picrate), N_1^+, N_2, and the acid proton is almost planar, with the latter proton just 0.04 Å out of the O^-, N_1^+, N_2 plane. This arrangement around the acid proton might be described as a three-center hydrogen bond.[19] However, the H–N_2 distance of 2.56 Å is only just about equal to the sum of the van der Waals radii, 1.0 Å for H[20a] and 1.55 for N.[20b] Hence, H···N_2 would be classified at best as a weak hydrogen bond. This type of N^+–H···N arrangement was also reported in Morse and Chesick's crystallographic study of *trans*-1,2-diaminocyclohexane monohydrobromide.[17]

(17) Morse, M. D.; Chesick, J. P. *Acta Crystallogr.* **1976**, *B32*, 954–956.
(18) Allen, F. H.; Kennard, O.; Watson, D. G.; Brammer, L.; Orpen, A. G.; Taylor, R. *J. Chem. Soc., Perkin Trans 2* **1987**, S1–S19.
(19) (a) Taylor, R.; Kennard, O.; Versichel, W. *J. Am. Chem. Soc.* **1984**, *106*, 244–248. (b) Jeffrey, G. A. In *Patterson and Pattersons: Fifty Years of the Patterson Function*; Glusker, J. P., Patterson, B. K., Rossi, M., Ed.; Oxford University Press: New York, 1987; pp 193–221.
(20) (a) Baur, W. H. *Acta Crystallogr.* **1972**, *B28*, 1456–1465. (b) Bondi, A. *J. Phys. Chem.* **1964**, *68*, 441–451.

Table III. pK_a Values for Diamines

compd	pK_{a1}	pK_{a2}	ref
1	10.6	3.3	*a*
2	10.5	4.4	*a*
3	11.1	3.3	*a*
4	10.9	5.3	*a*
5	10.8	3.7	*a*
4,5-diaminocyclohexene	9.9	6.6	*b*
ethylenediamine	9.89	7.08	*b*
1,3-Diaminopropane	11.11	10.11	*b*
2-amino-6-chloroaniline	3.94	0.6	*b*

[a] This work. [b] Summarized in ref 22.

Acidity constants of few cis vicinal diamines are known. One can imagine that intramolecular interactions via hydrogen bonds, N^+–H···N, in monoprotonated diamine together with repulsion between the nitrogens in diprotonated diamine render the second pK_a much smaller than the first. This is borne out qualitatively by our data in Table III. Concentration acidity constants were determined potentiometrically in 50% ethanol–water for several cis vicinal diamines.[21] In every case the two pK_a's differ by between 5 and 6 pK units, the larger pK_a being typical of that found for mono tertiary amines.[22] As seen among the examples in the table, this difference becomes less pronounced with increasing distance between the nitrogens. That the first pK_a's are so similar to values for simple tertiary amines may imply that intraspecies hydrogen bonding N^+–H···N is not a strong interaction. These data are consistent with the crystallographic results presented for **1**-picrate.

Both proton and ^{13}C NMR of **1** in cyclopentane-d_2 is essentially unchanged within the temperature range 150–300 K, the methyl resonance consisting of a single line in both NMR experiments. Then one can assume that the inversion rate at nitrogen is still fast relative to the NMR time scale even at 150 K. In contrast, salts containing monoprotonated **1** in CD_2Cl_2 exhibit major changes in ^{13}C NMR line shape between 190 and 250 K, especially that of the *N*-methyl resonance. In the case of the trifluoroacetate in CD_2Cl_2, the latter decoalesces to an equal doublet on cooling the sample to 190 K; see Figure 11. Similar effects were seen in ^{13}C NMR of the picrate and triflate salts at different concentrations as well as in proton NMR of the trifluoroacetates $IH^+CF_3CO_2^-$ and $ID^+CF_3CO_2^-$; see Table III. Proton NMR of *N*-methyls in both these salts consisted of equal doublets, separation 27 Hz. This is clearly the result of a chemical shift. Proton–proton coupling, $^3J(HN^+CH_3)$, was not observed in any of these salts; see below.

The carbinyl carbons in salts of **1** are chiral centers, so under conditions of slow inversion at nitrogen the *N*-methyl ^{13}C NMR should consist of two doublets, each of diastereotopic origin. We assume these salts take the unsymmetrical structure found for the picrate salt by crystallography, described above. That only one *N*-methyl doublet is observed for salts of **1** in ^1H and ^{13}C NMR must be the result of fast intramolecular proton transfer between nitrogens (4), fast with respect to the NMR time scale at 190 K. The signal averaging of the N–CH_3 ^{13}C doublet

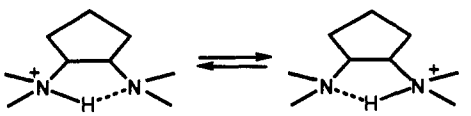

(4)

observed above 190 K is phenomenologically the result of inversion at nitrogen accompanied by rotation around the N–ring bond. The mechanism responsible must involve disruption of the N^+–H···N bond, most likely fast reversible proton transfer to trifluoroacetate counterion. No other proton acceptor is present in high concentration.

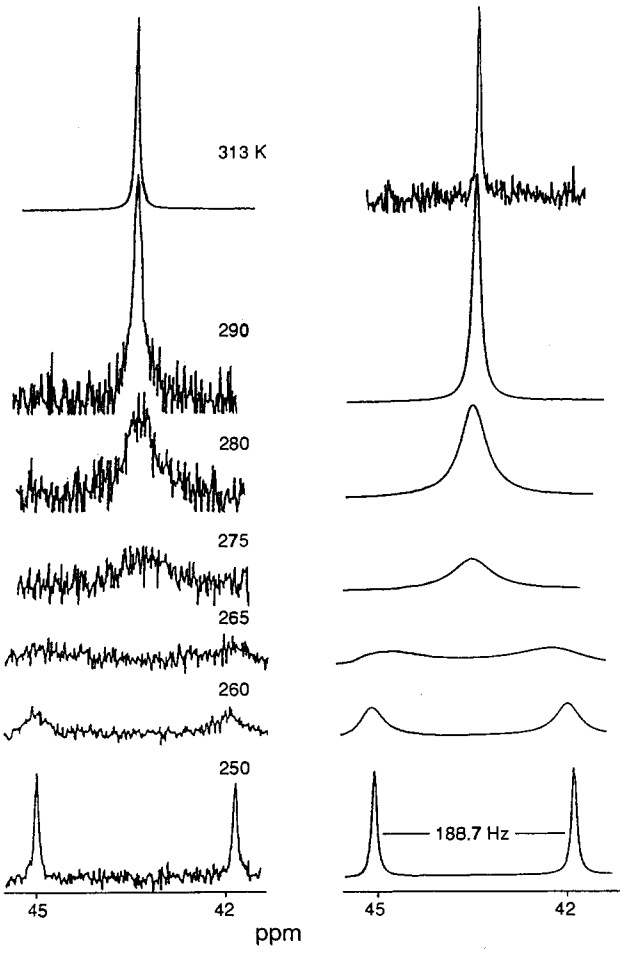

Figure 11. ^{13}C NMR, methyl line shapes of **1**–$H^+{\cdot}CF_3CO_2^-$ in CD_2Cl_2: (left) observed, different temperatures; (right) calculated.

Line-shape analysis of the ^{13}C *N*-methyl resonance, Figure 11, provides the specific rates of inversion at nitrogen, k_s. The corresponding Eyring plot is shown in Figure 12, giving $\Delta H_s^\ddagger$ = 22 kcal/mol and $\Delta S^\ddagger_s$ = 34 eu. The latter $\Delta S^\ddagger$ value would be consistent with our proposed rate-determining proton-transfer mechanism. In the following treatment, we assume that the salt **1**–$H^+CF_3CO_2^-$ (BH^+A^-) is ion-paired in CD_2Cl_2 and that its concentration greatly exceeds that of free diamine. Following Saunders and Yamada the total specific rate of nitrogen inversion in the sample, k_s, is given by[23]

$$k_s = \frac{k_i(B)}{[B] + [BH^+A^-]} \tag{5}$$

where k_i is the first-order rate constant for inversion of free diamine. Then taking into account eq 6 and dissociation of **1**–$H^+CF_3CO_2^-$, eq 7, and assuming that [B] = [HA], k_s is given by eq 8. Hence, the large positive value of $\Delta S_s^\ddagger$ (eq 9) is consistent

$$B \overset{k_i}{\rightleftarrows} B^* \tag{6}$$

$$BH^+A^- \overset{K_a}{\rightleftarrows} B + HA \tag{7}$$

$$k_s = k_i K_a^{1/2}[BH^+A^-]^{-1/2} \tag{8}$$

with the proposed mechanism; it would be due to the effect of

(21) Alberts, A.; Seargent, E. P. *The Determination of Ionization Constants*, 3rd ed.; Chapman and Hall: London, 1984.
(22) Listed in the following: Smith, R. M.; Martell, A. E. *Critical Stability Constants*; Plenum Press: New York, 1975, pp 36–35.
(23) (a) Saunders, M.; Yamada, F. *J. Am. Chem. Soc.* **1963**, *85*, 1882. (b) Morgon, W. R.; Leyden, D. E. *J. Am. Chem. Soc.* **1970**, *92*, 4527.

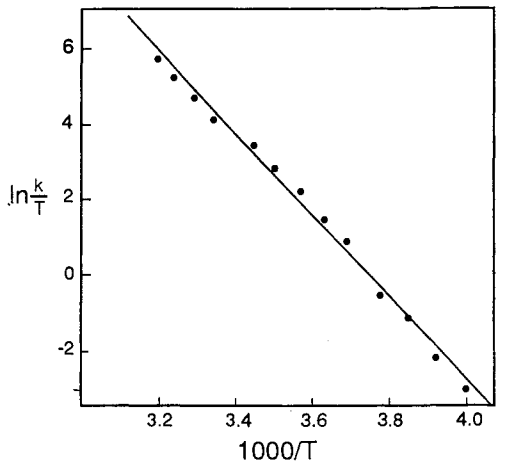

Figure 12. Eyring plot for nitrogen inversion in 1-H$^+$·$CF_3CO_2^-$ in CD_2Cl_2.

Table IV. Proton NMR Shifts (δ) for 1-H$^+$A$^-$ in CD_2Cl_2

^{1}H NMR

A$^-$	N$^+$–H(D)	*T* (K)	N*CH*$_3$	*CH*	*CH*$_2$CH–*CH*$_2$(CH$_2$)$_2$
$CF_3CO_2^-$	H	303	2.96	4.07	1.98–2.36
$CF_3CO_2^-$	H	230	2.987	4.05	2.03–2.28
			2.879		
$CF_3CO_2^-$	D	303	3.00	4.05	2.04–2.30
	D	240	3.017		
			2.917		
picrate	H	303	2.57	3.19	1.98–2.11
picrate	H	200	2.46	3.12	1.83–2.09
$CF_3SO_3^-$	H	303	2.68	3.37	1.92–1.97
$CF_3SO_3^-$	H	190	2.51	3.15	1.68–1.95

^{13}C NMR

A$^-$	N$^+$–H(D)	*T* (K)	N*CH*$_3$	*CH*	*CH*$_2$CH	*CH*$_2$(CH$_2$)$_2$
$CF_3CO_2^-$	H	303	44.26	68.32	25.05	20.05
$CF_3CO_2^-$	H	230	44.943	67.03	24.21	19.84
			41.749			
$CF_3CO_2^-$	D	303	44.20	68.28	24.91	20.27
$CF_3CO_2^-$	D	250	45.306	67.45	24.37	19.90
			42.093			
picrate	H	313	44.21	68.29	25.32	21.83
picrate	H	190	45.33	66.45	23.81	20.88
	H		41.04			
$CF_3SO_3^-$	H	303	44.13	67.94	25.13	21.49
		190	45.146	66.17	24.06	20.86
			41.20			

desolvation on ΔS_a for reaction 7 since ΔS_i^* (for inversion) should be close to 0. Further kinetic studies will clarify in further detail

$$\Delta S_s^* = \Delta S_i^* + {}^1/_2\Delta S_a \qquad (9)$$

the mechanism of nitrogen inversion in these salts, especially the relative timing of hydrogen bond cleavage and proton transfer to counterion.

As indicated above and in Table IV, other salts of **1** behave qualitatively in similar fashion to the trifluoroacetate. However, the observed rates of amine inversion are different. That should not be surprising since these are different ion pairs, and the proposed mechanism involves a proton transfer within the ion pair.

Assuming that the cations in the salts of **1** have similar structures in CD_2Cl_2 solution to that determined crystallographically for the picrate, the fast intramolecular proton transfer must be accompanied by a conformational flip of the N_1–C_1–C_2–N_2 assembly. It is interesting that proton transfer between the nitrogens is so much slower in the crystal compared to CD_2Cl_2 solution.

While the lifetime of the ion pair 1-H$^+$$CF_3CO_2^-$ cannot be measured, its lower limit would be the mean lifetime between successive inversions. At 250 K that is 0.08 s. The weak hydrogen bond from N$^+$–H to neutral nitrogen may help account for the long lifetime of the ion pair.

Table V. Crystallographic Details, 1-Picrate

formula	$C_9H_{21}N_2^+C_6H_2N_3O_7^-$
fw	385.38
space group	*C*2/*c*
a, Å	20.751(3)
b, Å	11.968(3)
c, Å	16.590(2)
β, deg	112.36(1)
V, Å^3	3811(1)
Z	8
d (calc), g/cm^3	1.34
cryst size, mm^3	0.19 × 0.27 × 0.31
radiation	Mo Kα with graphite monochromator
linear abs coeff, cm^{-1}	1.01
temp	ambient
2θ limits	$4° \le 2\theta \le 50°$
data collected	$+h,+k,\pm l$
unique data	3538
unique data with $F_o^2 > \sigma(F_o^2)$	1334
final no. of variables	248
$R(F)^a$	0.063
$R_w(F)^b$	0.058
goodness-of-fit	1.60

^{a} $R(F) = \Sigma||F_o| - |F_c||/\Sigma|F_o|$. ^{b} $R_w(F) = [\Sigma w(|F_o| - |F_c|)^2/\Sigma w|F_o|^2]^{1/2}$, with $w = 1/\sigma^2(F_o)$.

Conclusions

Data presented on the behavior and structure of cyclic cis vicinal tertiary diamines shows Eyring activation parameters for chair–chair interconversion in cyclohexane and piperidine moieties to be quite similar to those found for cyclohexanes and piperidines alone. X-ray crystallography of **1**-picrate reveals diamine **1** to be unsymmetrically protonated. In solution, proton transfer between nitrogens in monoprotonated **1** is fast on the NMR time scale at 170 K, while proton transfer between ammonium cation and counterion is considerably slower.

Experimental Section

Proton, 250-MHz, and ^{13}C, 62.986-MHz, NMR data were obtained using the Bruker AM250 spectrometer equipped with a temperature control and a deuterium lock. Gas chromatography was handled with a Hewlett-Packard HP-5710A instrument with a flame ionization detector and a 12-m glass capillary column, i.d. 0.2 mm, coated with SP2100 liquid phase. pK_a's were determined by acidimetric titration under argon in 50% ethanol–water using a Radiometer-Copenhagen pH meter equipped with a Fisher Accuphast (13-369-380) combination electrode. Diamines used in this work were prepared as reported by us previously. A modification of the preparation of **1** is described below.

X-ray Crystallography of 1-Picrate. The crystal used for data collection was clear, yellow-orange, and chunk-like in form with well-defined faces. Preliminary examination of the diffraction pattern on a Rigaku AFC5 diffractometer indicated a monoclinic crystal system with systematic absences: hkl, $h + k = 2n + 1$, and $h0l$, $l = 2n + 1$, which limit the space group possibilities to *C*2/*c* and *Cc*. At room temperature the unit cell constants were determined from a symmetry-restricted least squares fit of the diffractometer setting angles for 25 reflections with 2θ values in the range 20–30° and with Mo Kα radiation; see Table V for parameters.

Intensities were measured by the ω–2θ scan method. The crystal stability was monitored during the course of data collection by the measurement of a set of six standard reflections after every 150 reflections; the crystal remained stable during this time. Data reduction and all further calculations were carried out with the TEXSAN package of crystallographic programs.[24]

The structure was solved with the direct methods program MITHRIL[25] in space group *C*2/*c*. This space group choice results in the asymmetric

(24) *TEXSAN, TEXRAY Structure Analysis Package*, Version 2.1; Molecular Structure Corporation: College Station, TX, 1987.

(25) Gilmore, C. J. *MITHRIL: A Computer Program for the Automatic Solution of Crystal Structures from X-ray Data*; University of Glasgow: Scotland, 1983.

unit containing the 1:1 complex, i.e., one molecule each of the picrate anion and diamine monocation. The picrate anion and most of the amino–ammonium cation were located on the electron density map. The picrate molecule was then used as a phasing model in DIRDIF,[26] and all of the positions of the non-hydrogen atoms of the diamine were then located. Full matrix least squares refinement of the model minimized the function $\sum w(|F_o|-|F_c|)^2$ with $w = 1/\sigma^2(F_o)$. After a cycle of anisotropic refinement, many of the hydrogen atoms were located on a difference electron density map, including the hydrogen atom bonded to N_1. The hydrogen atoms were included in the model as fixed contributions in calculated positions with a C–H bond length of 0.98 Å and $B(H) = 1.2\,B_{eq}(C)$. The methyl hydrogen atoms were idealized to sp^3 geometry based on their positions as located on various difference electron density maps. Only the hydrogen atom bonded to N_1 was allowed to refine (both position and isotropic thermal parameters), and its final position is very close to its original position on the difference electron density map. The final refinement cycle for the 1334 intensities with $F_o^2 > 1\sigma(F_o^2)$ and the 248 variable parameters resulted in agreement indices of $R = 0.063$ and $R_w = 0.058$. A structure factor calculation for the 1089 reflections with $F_o^2 > 3\sigma(F_o^2)$ gives an R value of 0.049. The final difference electron density map contains maximum and minimum peak heights of 0.24 and –0.19 e/Å^3. Scattering factors were obtained from the usual sources.[27] The anisotropic displacement parameters for C_3, C_4, and C_5 are rather large and may indicate a disordering of the cyclopentane ring.

***cis*-1,2-Bis(*N*,*N*-dimethylamino)cyclopentane, 1.** A 500-mL Schlenk flask equipped with a stir bar and two 2-mm straight bore stopcocks, each protected with a serum cap, was flame dried in a current of argon and then loaded by syringe with 300 mL of cyclopentane and 2-(dimethylamino)cyclopentanone (7.6 g, 0.06 mol). After this assembly was cooled to –78 °C, dimethylamine (15.8 g, 0.35 mol) was introduced from a precooled (dry ice) syringe, followed by a solution of titanium tetrachloride (3.3 mL, 5.65 g, 0.0298 mol) in 12 mL of cyclopentane cannulated from a graduated cylinder under an argon atmosphere. By the time addition of the $TiCl_4$ was complete, a large quantity of green material had precipitated. The reaction mixture was stirred at –78 °C for 3 h more, then allowed to warm to room temperature, and stirred overnight for 10 h. By then a gray precipitate had separated, leaving a light yellow solution. This mixture was filtered through one layer each of Celite and Na_2SO_4, the two packed into a glass frit (25–50 μm) funnel. The gray yellow filtrate, cyclopentane solution of amino enamine, was transferred by syringe under argon to a flame-dried Parr jar together with 0.92 g of 5% Pd on carbon, and the assembly was flushed again with argon for 3 min. This system was hydrogenated at 50 psi. Consumption of H_2 was largely over after 30 min, but the system was allowed to run overnight to complete the reaction. After filtration of the catalyst and removal of cyclopentane, the residue was vacuum distilled, bp 41–43 °C/0.15 Torr, giving 9.3 g of **1**, a clear colorless liquid in 66.3% yield: ^{1}H NMR (300 MHz) δ units, CH 2.55–2.4 (m 2H), CH_3 2.18 (s 12H), CH_2 1.8–1.4 (m 6H); ^{13}C NMR (75 MHz) δ units, *C*H 68.73, CH_3 44.28, CH_2 25.96 and 22.00.

***cis*-1,2-Bis(*N*,*N*-dimethylamino)cyclopentane Monopicrate, 1-Picrate.** Diamine **1** (0.2 g, 0.001 28 mol) was dissolved in 5 mL of ethanol in a 25-mL Erlenmeyer flask. A saturated solution of picric acid in ethanol (6.2 g/100 mL) was prepared, and 4.74 mL of it, equivalent to the amount of diamine used, was added to the diamine solution. The resulting solution was heated to boiling for approximately 3 min. Then it was cooled to room temperature and further cooled in an ice bath. The product was powdery and thus not suitable for X-ray crystal analysis.

This product was redissolved in 6 mL of acetonitrile–ethanol (9:1), and the solution was warmed to 50 °C. The crystals started to grow very slowly as the solution was slowly cooled to room temperature. After standing at room temperature for approximately 5 h, the average size of the crystals was nearly 1 mm in diameter. The final picrate salt crystals were yellow and translucent. The X-ray crystal analysis was then carried out.

Acknowledgment. This research was supported in part by National Science Foundation Grant No. CHE 8717746, as was purchase of the high-field NMR equipment used in this work. We are happy to acknowledge technical advice from Dr. Charles Cottrell, Campus Chemical Instrumentation Center, and helpful discussions with Professor Daniel Leussing, Department of Chemistry, both at The Ohio State University.

Supplementary Material Available: Atomic coordinates and all structural parameters and experimental details relevant to the X-ray crystallography of the monopicrate of compound **1** (16 pages); listing of observed and calculated structure factors for the monopicrate of compound **1** (10 pages). Ordering information is given on any current masthead page.

(26) Beurskens, P. T. DIRDIF: Direct Methods for Difference Structures—An Automatic Procedure for Phase Extension and Refinement of Difference Structure Factors. Technical Report 1984; Crystallography Laboratory: Toernooiveld, 6525 Ed., Nijmegen, The Netherlands.

(27) Scattering factors for the non-hydrogen atoms are from the following: *International Tables for X-ray Crystallography*; Kynoch Press: Birmingham, England; Vol. IV, p 71. The scattering factor for the hydrogen atom is from the following: Stewart, R. F.; Davidson, E. R.; Simpson, W. T. *J. Chem. Phys.* **1965**, *42*, 3175–3187.